

See discussions, stats, and author profiles for this publication at:
<https://www.researchgate.net/publication/256421515>

Intermittencies and power-law low-frequency divergencies in a nonlinear oscillator

ARTICLE *in* PHYSICA D NONLINEAR PHENOMENA · JUNE 1989

Impact Factor: 1.64 · DOI: 10.1016/0167-2789(89)90250-9

CITATIONS

16

READS

5

3 AUTHORS, INCLUDING:



Miguel Angel Rubio

National Distance Education University

74 PUBLICATIONS 1,378 CITATIONS

[SEE PROFILE](#)



José Carlos Antoranz

National Distance Education University

118 PUBLICATIONS 1,021 CITATIONS

[SEE PROFILE](#)

INTERMITTENCIES AND POWER-LAW LOW-FREQUENCY DIVERGENCIES IN A NONLINEAR OSCILLATOR

M.A. RUBIO, M. DE LA TORRE* and J.C. ANTORANZ

Departamento de Física Fundamental, Universidad Nacional de Educación a Distancia, Aptdo. Correos 60141,
E-28080 Madrid, Spain

Received 7 September 1988

Accepted 28 November 1988

Communicated by Y. Pomeau

We have studied the different intermittent regimes in a nonlinear quadratic oscillator. By means of analog electronic simulations the intermittency region has been located in parameter space. The power spectrum exhibits a $1/f^\alpha$ behavior, with $\alpha = 1.2$. The intermittent region has been numerically studied and two different bifurcation schemes leading to Pomeau–Manneville intermittencies of type-I and type-III have been identified. Furthermore a continuous change in the slope of the power-law low-frequency power spectrum has been found and interpreted in terms of competition between two unstable fixed points. Finally, a one-dimensional map which displays the whole phenomenology of the physical system is provided.

1. Introduction

In the past recent years a new concept has been developed in the theory of dynamical systems which has a great importance for its implications in the understanding of the transition to weak turbulence. This new concept has been called deterministic chaos, and stands for the unpredictability of the behavior of nonlinear dynamical systems even with a reduced number of degrees of freedom [1, 2]. It has been shown that this deterministic chaos can be attained by several routes [3], and one of the major goals in this field has been to state some universal characteristics that would allow to identify the final states reached through every one of these routes [4–6].

One of the properties that has received much attention in these studies is the power spectrum of

the systems undergoing this type of behavior [7]. Since the very beginning the broadening of the spectral lines and the enhancing of the noise were recognized as signatures of the presence of deterministic chaos [8], but soon after special attention was given to the amazing low-frequency phenomena appearing in these systems. In particular the occurrence of power-law low-frequency divergencies has been extensively studied, both theoretically [9–11] and experimentally [12–15].

Most of these studies have been performed on very simple dynamical systems, namely forced oscillators. The Duffing oscillator and the driven damped pendulum or its Josephson-junction analog are the most popular among them. Some of these systems have recently received more relevance due to their appearance as normal forms in codimension-two bifurcation theory, e.g., the Duffing–Van der Pol oscillator [16].

One of these systems is the so-called Helmholtz oscillator [17], which is a driven damped oscillator with a quadratic nonlinearity in the restoring force.

*Present address: Dept. Theoretische Physik IV, Universität Bayreuth, NW II, 8580 Bayreuth, Fed. Rep. Germany.

It was proposed by Helmholtz to explain the combinational tones generated in the eardrum, and it has added interest because it is a canonical form in catastrophe theory [18, 19]. Besides that, a previous analog simulation work [20] showed some kind of intermittent behavior in this oscillator, although a complete identification of this state could not be performed.

Systems like the Helmholtz or Duffing oscillators can show only one fundamental frequency in their evolution and therefore the universal scenarios of transition to chaos to be expected are the well-known period-doubling cascade [21] and the type-I and type-III Pomeau–Manneville intermittencies [22] (a system with higher-dimensional phase space would be needed to have type-II intermittency [23]). Here we provide complete numerical results which prove that in the Helmholtz oscillator a continuous transition between the two possible types of intermittency exists. We also report new results on an anomalous power-law behavior in the low-frequency part of the power spectrum in type-I intermittency. Variations of the power-law exponent with the control parameter have already been found in other systems [13c, 15]. In our system this behavior is shown to be caused by the competition between two unstable fixed points.

The paper is organized as follows. In section 2 we briefly describe the model system and report on some analog simulations performed to locate the interesting regions in parameter space. In section 3 the numerical results yielding different bifurcations in parameter space are presented. Besides, bifurcations to both types of intermittency are characterized and the above-mentioned continuous transition is discussed. In section 4 the power spectra for both types of intermittent regimes are presented and compared to theoretical predictions. Furthermore, the anomalous behavior found for type-I intermittency is explained. In section 5 we introduce a seventh order polynomial discrete map that reproduces the dynamical properties of our system. Finally, the conclusions are stated in section 6.

2. The model system

2.1. The Helmholtz oscillator

As already sketched in the introduction the Helmholtz oscillator was presented as a reduced model to explain the vibrations of a pre-stressed membrane. In order to explain the combinational tones in the eardrum a quadratic nonlinearity was introduced in the equation corresponding to a driven damped oscillator. Therefore the potential involved (see fig. 1(a)) is an asymmetric cubic potential having only one attracting region which allows the system to escape to *minus infinity* under

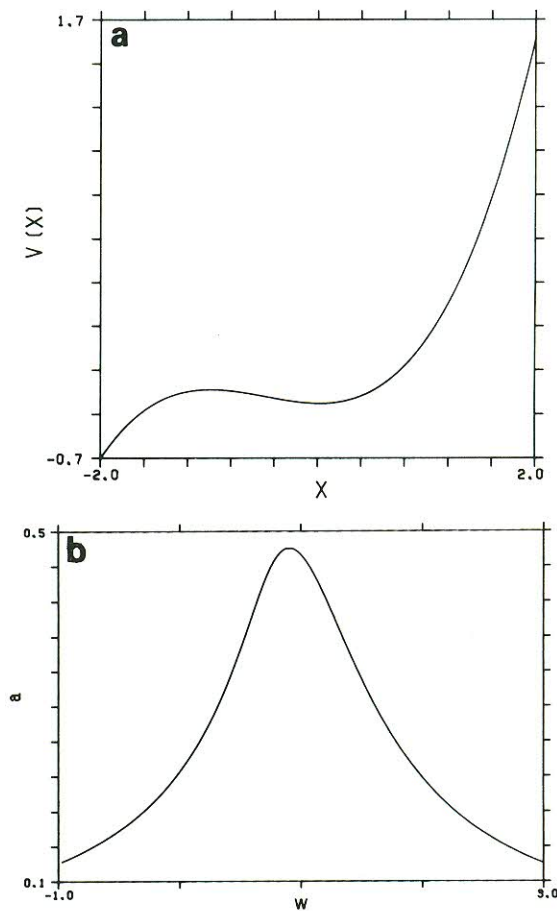


Fig. 1. (a) Potential well for the Helmholtz oscillator. (b) Nonlinear resonance curve for $g = 0.52$ and $A = 0.5$ (a is the oscillation amplitude).

certain conditions. The actual equation that rules the dynamics of the system, with time normalized with respect to the natural period of the linear oscillations, is

$$\frac{d^2x}{dt^2} + g \frac{dx}{dt} + x + x^2 = A \cos \omega t,$$

where g , ω and A stand, respectively, for the damping coefficient, the frequency and the amplitude of the forcing term. For this oscillator the resonance response curve can be calculated [24] and is shown in fig. 1(b), where a is the amplitude response. The general expression for this nonlinear response shows that it is a *soft* oscillator independent of the sign of the nonlinear term. This means that the resonance curve always bends toward frequencies lower than the natural one (here $\omega = 1$). This implies that for frequencies higher than 1 there is a *single* stable limit cycle of period $T = 2\pi/\omega$.

In what follows, to avoid hysteretic phenomena due to the existence of two T -period stable limit cycles, we have chosen as working region the one corresponding to $\omega > 1$.

2.2. Analog simulation results

In order to locate the interesting regions in parameter space in an efficient way we built up an electronic analog simulator. This simulator was made up with two Miller integrators and used as nonlinear element a four quadrant analog multiplier, namely an AD533 integrated circuit.

The periodic forcing was provided by an Interstate F30 signal generator with variable frequency. The amplitude of the forcing and the actual value of the damping coefficient could be adjusted with two multturn potentiometers. The signals corresponding to variables x and dx/dt were sent to an oscilloscope where phase space evolution could be examined.

Furthermore, both signals were fed into a Spectral Dynamics SD375 Fourier analyzer. Pictures of

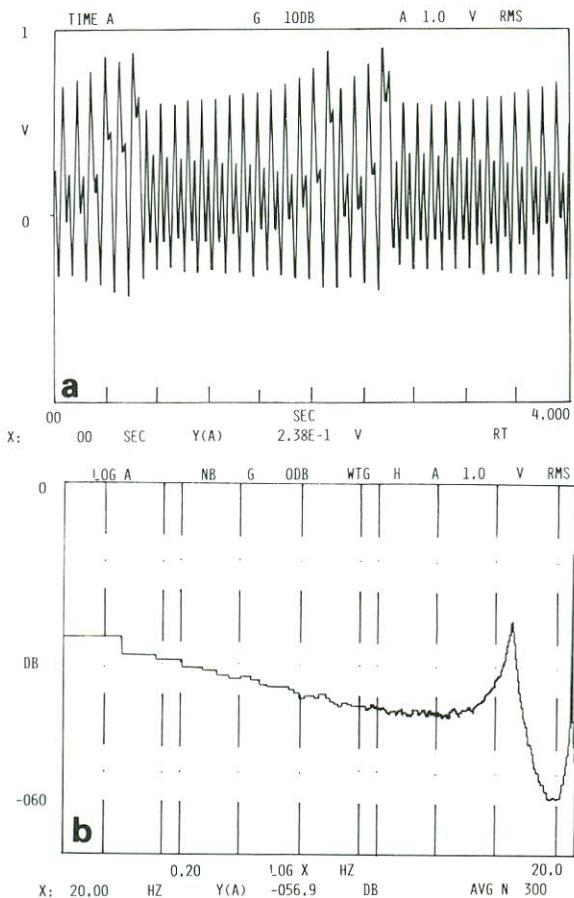


Fig. 2. Time evolution (a) and corresponding averaged power spectrum (b) of the analog simulator signal for $g = 0.52$, $\omega = 1.3$, and $A = 0.5$. The spectrum has been averaged over 300 times and it yields $\alpha = -1.2 \pm 0.1$.

the time evolution and averaged power spectra of the simulator output were directly obtained through a digital plotter HP7470. For moderately high damping ($g > 1$) the usual bifurcation schemes that appeared were period doubling cascades. For $g < 1$ some regions with intermittent regimes were found for $1.2 < \omega < 1.4$.

In particular the most interesting region was located around $g = 0.52$ and $\omega = 1.3$. For this value an intermittent signal with power-law low-frequency behavior was found. The experimental results are depicted in figs. 2(a) and 2(b). Fig. 2(a) corresponds to the time evolution of variable x for

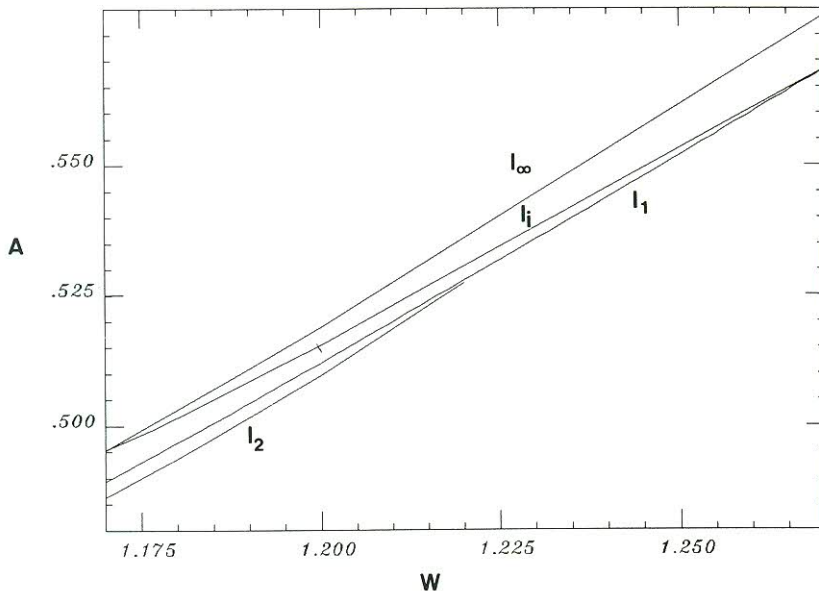


Fig. 3. Regions of periodic and chaotic solutions in parameter space for $g = 0.52$. l_∞ – boundary for evolution inside the potential well. l_i – supercritical period doubling. l_i – bifurcation from period $2T$ to chaos. l_2 – relaxation of the chaotic attractor of the subcritical branch to the T -periodic regime.

$g = 0.52$, $\omega = 1.3$ and $A = 0.5$. As can be seen a clear intermittent behavior is present. Its corresponding power spectrum, plotted in fig. 2(b) in log-log scale, averaged over 300 times, shows a definite $1/f^\alpha$ trend over two decades with an exponent α around -1.2 ± 0.1 . Both the time evolution waveform and the exponent in the power-law divergence would lead to label this intermittency as type-III [10, 25]. Needless to say, this low-frequency noise had in our circuit a clear dynamical origin, because the corresponding noise in periodic regimes was three orders of magnitude lower.

We however point out that this type of behavior always appeared for values of A driving the system very close to escape from the attracting region of the potential. This situation lead to problems in the stability of the system, that together with the accuracy of the parameter setting made unfeasible more detailed studies of the bifurcation leading to this intermittent regimes. Therefore we performed a thorough numerical study of the bifurcations appearing in the previously cited zone of parameter space.

3. Intermittency in the Helmholtz oscillator

We carried out a detailed study of the parameter space in the region indicated by the analog simulations. All computations have been performed with a fourth order Runge–Kutta method with double precision arithmetics, and time step of 0.01 that proved to be sufficient for our purposes. In fig. 3 we plot the critical point curves corresponding to the main bifurcations in the plane ω – A for $g = 0.52$.

We have labeled these curves as follows. Curve l_∞ is the limit of bounded evolution inside the single well potential, i.e., when this line is crossed to the upper left part the system escapes to *minus infinity*.

Curve l_i is the stability boundary for the T -periodic solution. At this curve a supercritical period doubling bifurcation occurs, and therefore a stable $2T$ -periodic solution is present beyond this line.

Curve l_2 is the stability boundary for this $2T$ -periodic solution. Beyond this curve no periodic attractor exists and the time evolution of the sys-

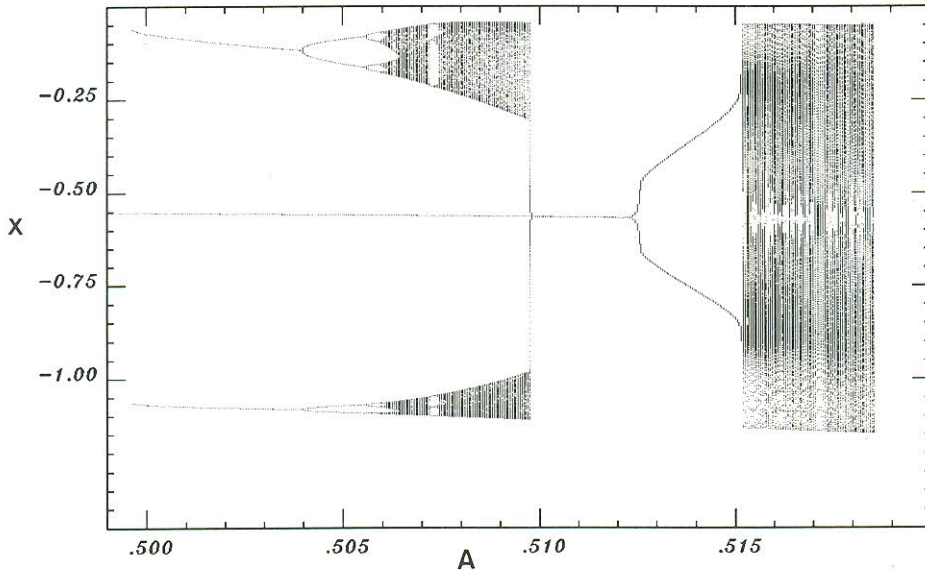


Fig. 4. Bifurcation map obtained for the minima of x for $g = 0.52$, $\omega = 1.2$. The intermittent bifurcation occurs at $A_1 = 0.51515$.

tem reveals features characteristic of intermittent regimes as well be shown soon after. We point out that this bifurcation shows no hysteretic behavior. Incidentally we can appreciate that for $\omega = 1.2$ the width of the region located among the supercritical period doubling and the escape to *minus infinity* is around 0.006 for the A parameter, thus explaining the difficulties in stabilizing the analog simulator in this region.

Finally curve l_2 represents the boundary of a chaotic attractor arising from another stable $2T$ -periodic solution that undergoes a complete subharmonic bifurcation cascade. More explicitly, below l_2 the chaotic attractor is stable while above this line, it relaxes to the stable T -periodic orbit (a scenario close to this has been discussed in [26]).

3.1. Type-I intermittency

We will first try to characterize the intermittent transition that takes place at curve l_1 . A typical bifurcation diagram is shown in fig. 4, where the values taken for ω and g are, respectively, $\omega = 1.2$ and $g = 0.52$. This bifurcation map has been ob-

tained by plotting the minima of $x(t)$ calculated in the following way. The control parameter A was varied in steps of 5.0×10^{-5} . Sufficient time was left for the system to arrive at a stable state after each A step (convergence of better than 10^{-5} was required). The final point for each value of A was taken as the initial condition for the following integration. The only exception to this rule concerning the initial conditions was made to locate the subcritical $2T$ -periodic branch. When the system finally escaped to *minus infinity* the final point for the previous A value was used as an initial condition to explore the bifurcation diagram descending in A . In this bifurcation map the previously cited bifurcations can be seen. There is a supercritical period doubling bifurcation at $A = 0.5122$ and the emerging $2T$ -periodic solution loses its stability at $A_1 = 0.51515$ where an intermittent regime appears. Upon decreasing A these two bifurcations show no hysteresis.

For different initial conditions another $2T$ -periodic solution can be found for lower values of A . This solution appears at $A = 0.4995$ and upon increasing A this orbit undergoes a complete pe-

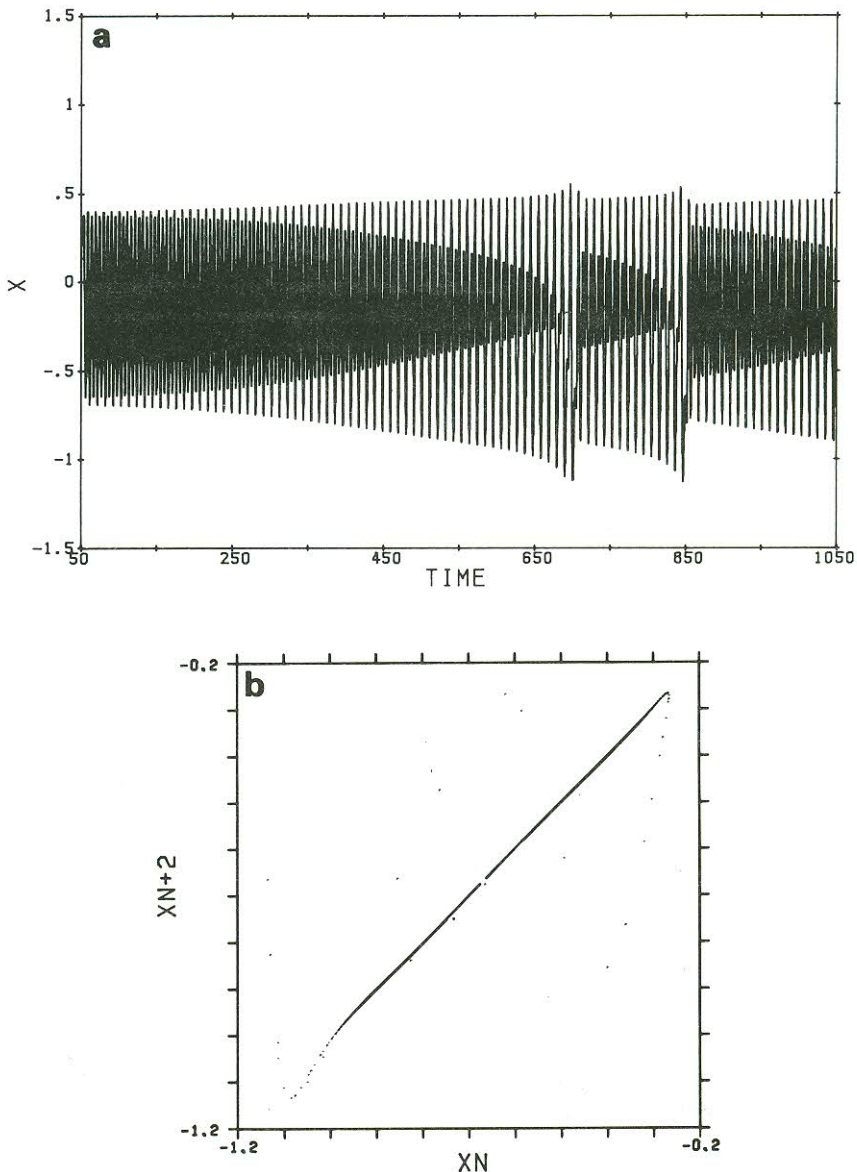


Fig. 5. Time evolution (a) and corresponding second iterate return map for the minima of x (b) at $g = 0.52$, $\omega = 1.2$ and $A = 0.5152$.

riod doubling sequence leading it into chaos. This chaotic attractor finally decays into the T -periodic solution prior to the supercritical period doubling bifurcation.

We were mainly interested in the intermittent regime appearing at A_1 . Its time evolution and second iterate return map are plotted in figs. 5(a) and 5(b). The time evolution shown in fig. 5(a), for

$A = 0.5152$, strongly resembles that in ref. [25]. A subharmonic of the driving frequency is present and its amplitude gradually increases until the appearance of a chaotic burst leading to another laminar region of different length.

Moreover, its corresponding second iterate return map, made with the minima of x (fig. 5(b)), shows a crossing of the bisector with positive

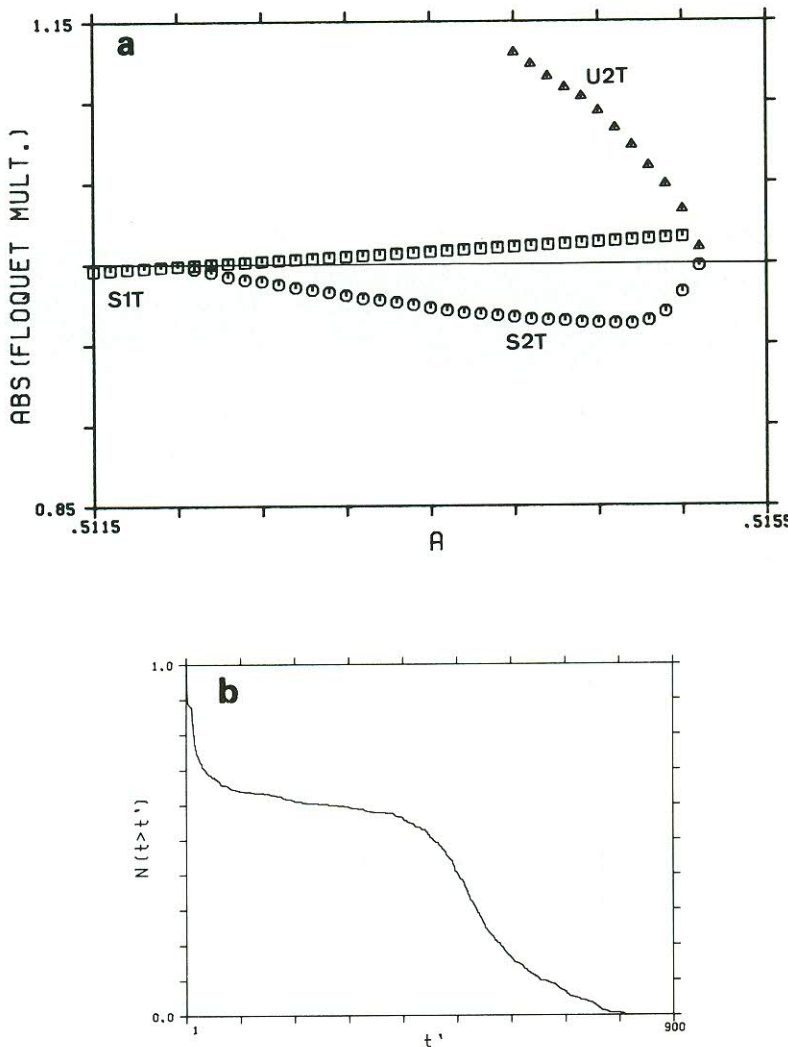


Fig. 6. (a) Absolute value of the Floquet multipliers for the T - and $2T$ -periodic orbits as functions of A near the intermittent bifurcation. Only the line corresponding to the T -periodic limit cycle has actual negative values. (b) $N(t \geq t')$ near the bifurcation ($A = 0.5152$).

slope. However this crossing happens at the point corresponding to the unstable T -periodic fixed point, so this slope higher than +1 cannot be used to label the intermittency found here as pertaining to type-I or type-III. Besides, the nonexistence of hysteresis upon decreasing A at the subcritical bifurcation is explained by the return map in fig. 5(b). It shows that in the chaotic branch for $A < A_1$ reinjections are allowed near the stable $2T$ -peri-

odic fixed point, and therefore relaminarization necessarily occurs after some time.

A definite identification of an intermittent regime can be done only by means of a study of the Floquet multipliers and statistical properties, such as the distribution of the laminar periods in the vicinity of the bifurcation point [22, 25]. Numerically the Floquet multipliers can be easily computed (see for example [27]) as a function of

A for all stable orbits and even when they get unstable. After the work of Pomeau and Manneville [28], the different types of intermittent behavior are classified according to the value of the Floquet multiplier at the bifurcation point. If a real Floquet multiplier crosses the unit circle at $+1$, corresponding to an inverse saddle-node bifurcation, then the intermittency is labeled as type-I. Conversely, if it crosses at -1 , corresponding to a subcritical period doubling, it is labeled as type-III.

Turning to the statistical properties, it is usual to study the probability distribution for the length of the laminar periods. In the case of type-I intermittency, its shape reveals two peaks, one for short laminar periods and another for higher lengths, corresponding to the long passages through the channel [29]. For type-III, it has a simpler exponentially decreasing shape [1].

However, for limited amounts of data, it is convenient to speak in terms of an integral of this function, namely representing the number of laminar periods whose length is equal to or higher than a certain time t' as a function of $t'(N(t \geq t'))$ [22, 25].

This function shows a different shape for both types of intermittency. For type-III it is an exponentially decaying function, whereas for type-I it has a certain sigmoid shape, i.e., it decays for short lengths, after it shows a certain plateau, and finally it has another decaying part for the maximal laminar period lengths.

Here we report studies on both the Floquet multipliers and the function $N(t \geq t')$. The results of these studies are plotted in figs. 6(a) and 6(b). In fig. 6(a) we show the dependence on A of the absolute value of the Floquet multipliers corresponding to the different orbits involved in the main bifurcation sequence. The line $S1T$ corresponds to the T -periodic solution. In this case the actual values taken by the Floquet multiplier are negative, therefore it crosses the unit circle at -1 , giving, then, a direct subharmonic bifurcation at $A = 0.5122$. The $2T$ -periodic orbit appearing in

this point is represented by $S2T$, with positive actual values. At $A = 0.51515$, this orbit crosses the unit circle at $+1$, colliding with another $2T$ orbit which is unstable ($U2T$). This gives rise to an inverse saddle-node bifurcation, at which the intermittent regime appears. Consequently, this regime can be unambiguously labeled as a type-I intermittency.

This conclusion has been also ascertained by the statistics of the system. In fig. 6(b) we have plotted the function $N(t \geq t')$ at $A = 0.5152$. Its shape is clearly the one that should be expected for type-I intermittency.

3.2. Type-III intermittency

The previously described intermittent transition is not the only one that can be found in the Helmholtz oscillator. For instance, a different type of bifurcation is shown in fig. 7. This bifurcation map was obtained in the same way as the former one but for $\omega = 1.3$ and $g = 0.48$.

The whole appearance of fig. 7 is very similar to that of fig. 4, but there is a crucial difference, i.e., the intermittent regime is attained directly from the T -periodic orbit, at a value of $A_{\text{III}} = 0.5610$. In this case the Floquet multiplier of the T -periodic solution crosses the unit circle at -1 , and there is not another stable periodic solution available to the system. Moreover, the system is under the influence of the subcritical period doubling giving rise to the upper and lower branches in the bifurcation map.

This analysis allows us to label this intermittent regime as pertaining to type-III intermittency. It is further confirmed by the second iterate return map, that in this case shows a slope slightly higher than $+1$ for the unstable fixed point undergoing this transition (fig. 8(a)). The study of the statistics of the laminar periods close to the bifurcation ($A = 0.5612$), leads to the same conclusion (see fig. 8(b)).

At this point we come back to compare numerical and analog results. At first sight the agreement

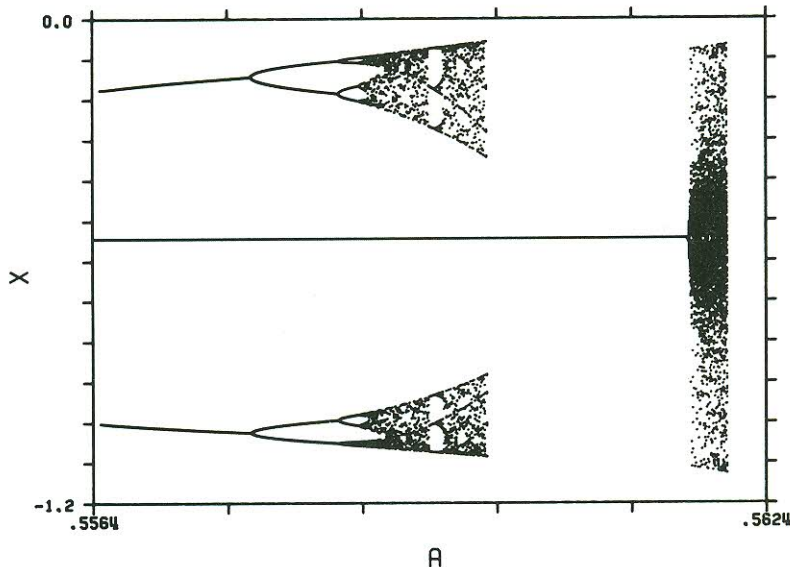


Fig. 7. Bifurcation map obtained for the minima of x for $g = 0.48$, $\omega = 1.3$. The intermittent bifurcation occurs at $A_{\text{III}} = 0.5610$.

seems quite satisfactory having in mind that our average absolute accuracy in the analog parameter values setting is around 1%. The difficulties in stabilizing the intermittent regime are also explained upon the narrowness of the intermittent regions in this zone of parameter space.

Nevertheless, with the analog simulator data at our disposal it was not possible to label the observed regime as belonging to type-I or type-III, because we could not perform studies on the statistics. So we studied the statistical properties of this regime taking into account only the low-frequency part of the power spectrum of the system.

4. Intermittency and $1/f$ noise

We have computed the power spectra corresponding to both types of intermittent regimes. For the parameter values giving rise to type-III intermittency ($A = 0.5610$, $\omega = 1.3$, $g = 0.48$), the computations yield plots as shown in fig. 9(a), where the spectrum has been averaged over 150

times. The power-law behavior is clear, and its slope was evaluated to be -0.96 ± 0.01 . This slope and the whole shape of the power spectrum turned out to be independent of A . This behavior is consistent with what should be expected for type-III intermittency [10] (logarithmic corrections for very low frequency are masked by the contribution of asymmetry respect to $x = 0$).

On the other hand the behavior for the type-I regime ($\omega = 1.2$, $g = 0.52$) is unusual. The general low-frequency behavior still shows a power-law region, but in this case the average slope turned out to be dependent on A . For instance, near the bifurcation ($A = 0.51517$) the slope was close to -1.14 . In fig. 9(b) we plot the power spectrum at $A = 0.5152$ at which the exponent α is 1.10. Upon further increasing A the slope still decreases. For instance, at $A = 0.517$, the slope turned out to be -0.97 ± 0.01 . There are reports in the literature on some similar changes in the slope of the power spectra [13c, 15], but this behavior seems far from being understood.

Another remarkable feature can be seen in fig. 9(c), for $A = 0.516$, in which a ripple appears

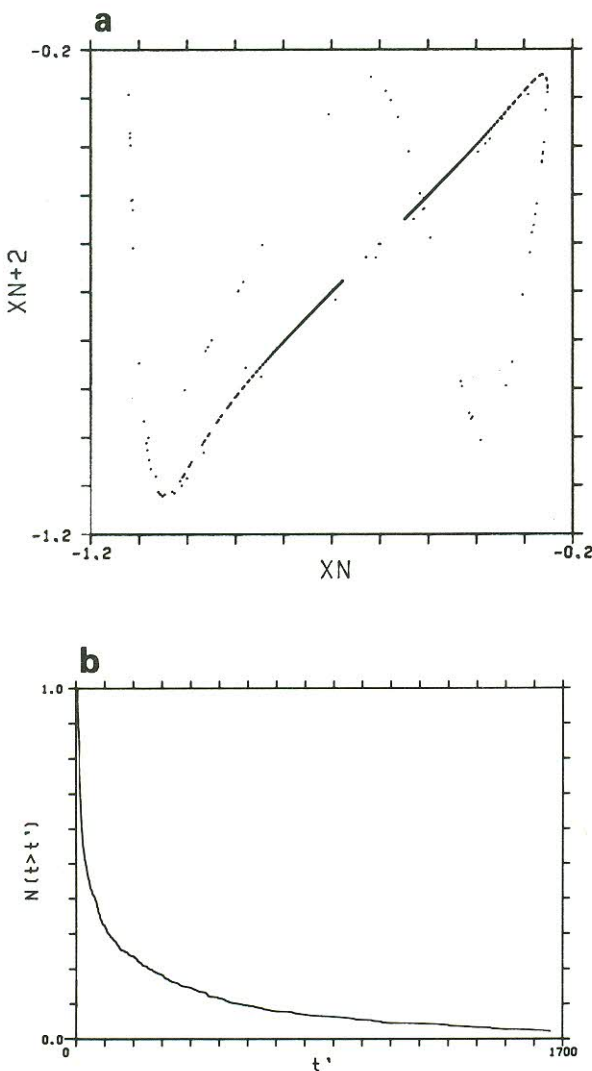


Fig. 8. Second iterate return map for the minima of x (a) and corresponding $N(t \geq t')$ (b) for $g = 0.48$, $\omega = 1.3$ and $A = 0.5612$.

superimposed to the power spectrum. This ripple disappears for $A > 0.5165$ (see, for example, fig. 9(d), at $A = 0.518$) giving rise to a flat portion in the lower frequencies, and another power-law region with exponent around 0.9. In our case the whole behavior can be explained in terms of the statistics and the return map of the system.

First of all, let us make a brief summary of the way in which the theoretical predictions of low-

frequency behavior are done [10]. For a given return map, each laminar period is substituted by a single event corresponding to its end. Further on, the time correlation function of this sequence of events is calculated and finally upon Fourier transforming, the power spectrum is obtained. It follows that the low-frequency part of the power spectrum is directly related to the longest laminar periods available to the system.

So, let us consider the statistical function $N(t \geq t')$ as a function of A . For instance, in figs. 6(b) and 10 we show this function for $A = 0.5152$ and $A = 0.518$. It can be observed that as A increases the maximal length of the laminar period decreases, as expected, and consequently the plateau shrinks. It produces a change in the general shape of the curve, monotonically approaching the type-III one.

In fact at $A = 0.518$ the curve can be fitted with the theoretical expression corresponding to type-III intermittency, inserting the value of the control parameter obtained by fitting the return map in the way used in [25]. This comparison is shown in fig. 10 and the points belonging to the numerical simulation are in good agreement with the corresponding theoretical curve. The return map has been fitted to a cubic polynomial yielding a coefficient of the linear term of 0.015. Upon inserting this value in the expression for $N(t \geq t')$, the continuous curve in fig. 10 was obtained.

The conclusion is that in this region of parameter space the behavior of the system gradually changes its features going from type-I to type-III intermittent regime. In this way the ripple in the power spectrum is generated in the type-I intermittent regime, which has a sharp peak in the distribution of laminar lengths near to the maximal one. This privileged length causes the appearance of small wide peaks in the power spectrum when the corresponding frequency falls inside the range of frequency analysis.

This explanation is reinforced by a careful inspection of the second iterate return map. Let us have a closer look to the separation rate of the return map with respect to the bisector. In the

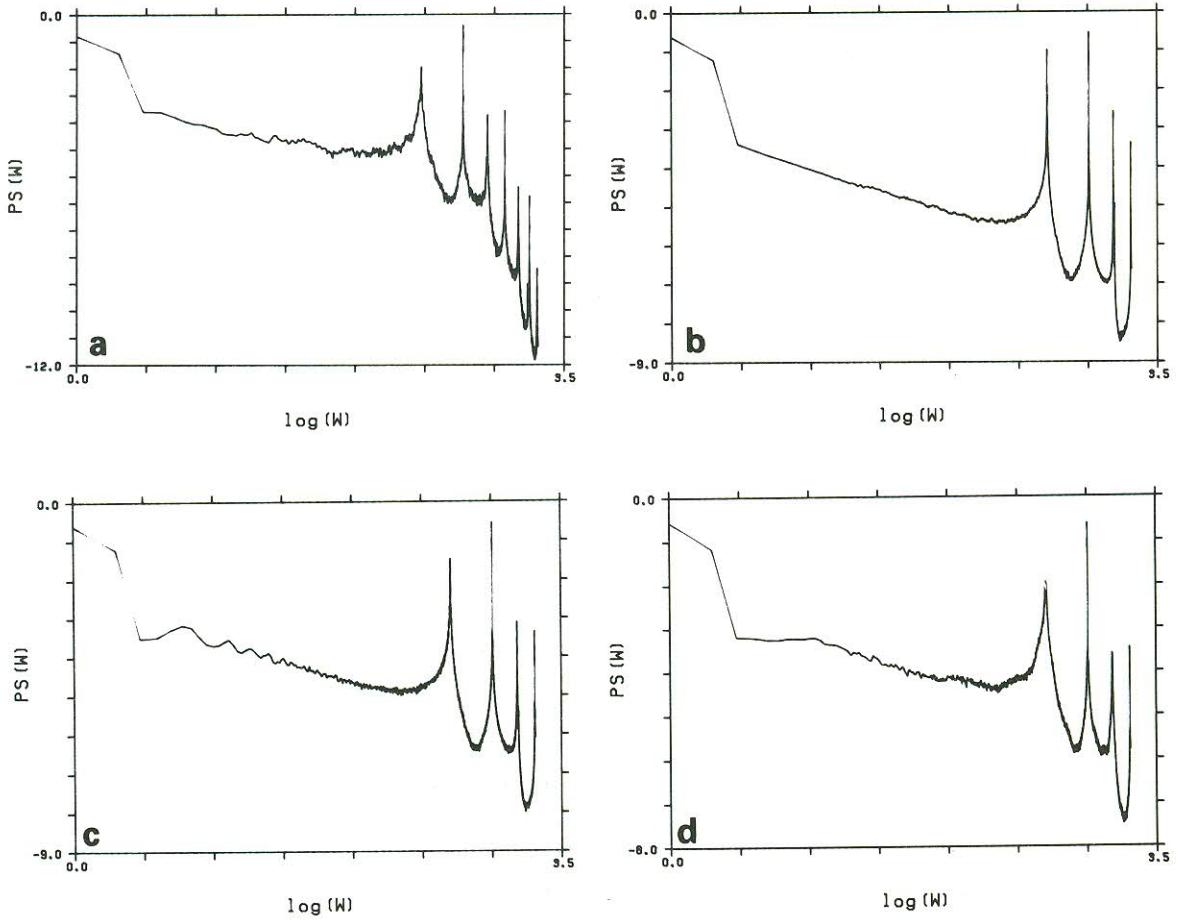


Fig. 9. Averaged power spectrum of x , at $g = 0.48$, $\omega = 1.3$, $A = 0.5612$ (a); and $g = 0.52$, $\omega = 1.2$ with $A = 0.5152$ (b), $A = 0.516$ (c) and $A = 0.518$ (d).

case of the type-III intermittent transition, the separation rate from the unstable T -periodic fixed point is a monotonically increasing function. However, in the type-I regime, the situation is different. For A values below the critical one, the return map presents three fixed points. One of the corresponds to the unstable T -periodic orbit. The other two belong to the couple of stable and unstable $2T$ -periodic orbits which will undergo the inverse saddle-node bifurcation. Therefore the return map crosses the bisector at three places. Two with slope higher than one, corresponding to the unstable fixed points, and one with slope smaller

than one corresponding to the stable $2T$ -periodic solution.

When the system undergoes the intermittent transition, the two $2T$ -periodic fixed points collide and disappear, leaving a hump in the return map, as sketched in fig. 11. Therefore the map presents only one unstable fixed point corresponding to the T -periodic orbit, but there is a reattachment of the map to the bisector corresponding to the previous $2T$ -periodic fixed points. In our system the global structure of the attractor allows for reinjection near the unstable T -periodic fixed point. Hence, the maximal length of the laminar regions will be

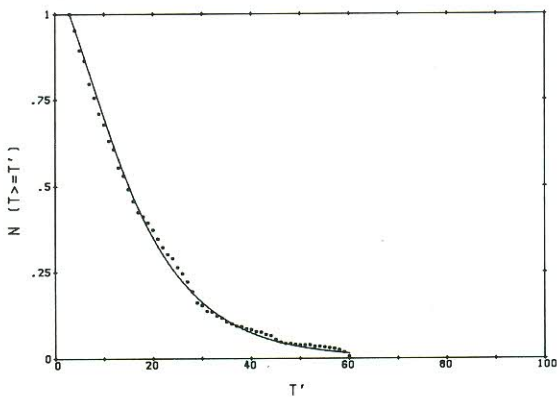


Fig. 10. $N(t \geq t')$ for $g = 0.52$, $\omega = 1.2$ and $A = 0.518$ (points) and corresponding type-III intermittency theoretical curve after least-squares fit of the return map (solid line).

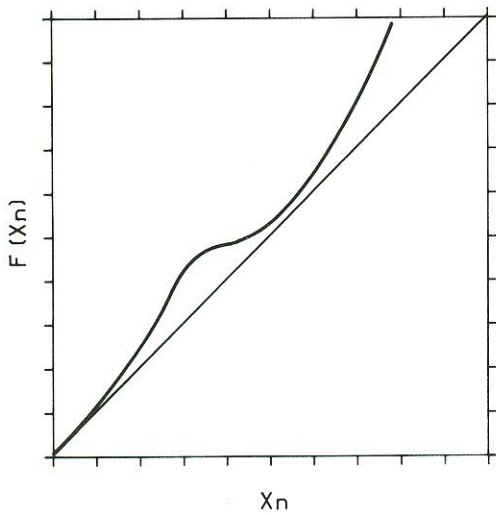


Fig. 11. Qualitative sketch of the return map yielding the behavior explained in the text.

ruled by the relative importance of the two processes involved: escape from the neighbourhood of the unstable fixed point and crossing the channel created by the intermittent transition.

Both processes may be analyzed in terms of the relative distance to the critical point, labeled by e . Escaping from the unstable fixed point is equivalent to a type-III intermittent regime and therefore, the average time required goes as e^{-1} .

Instead, for the type-I channel crossing, the maximal length goes as $e^{-1/2}$.

In our system, when the type-I intermittent transition takes place, the return map has a certain slope near the unstable T -periodic fixed point, but the width of the channel can be made arbitrarily small, therefore giving a behavior with type-I features, including exponent with modulus higher than one in the low-frequency spectrum. As A increases the hump goes away from the bisector faster than the slope near the unstable fixed point increases. Therefore the behavior of the system approaches that corresponding to type-III intermittency. In this way the modulus of the power law's exponent decreases.

Incidentally, we point out that when the hump goes away from the bisector, the region of the map between the hump and the unstable fixed point is nearly parallel to the bisector, therefore inducing a flat portion in the power spectrum (see ref. [10]).

However, in the case of the Helmholtz oscillator, the slope change in the power law is small. This is caused by the fact that very near to the bifurcation point, the laminar periods become very long, therefore giving contributions to frequencies exceedingly low to be analyzed with the usual numerical Fourier transforms.

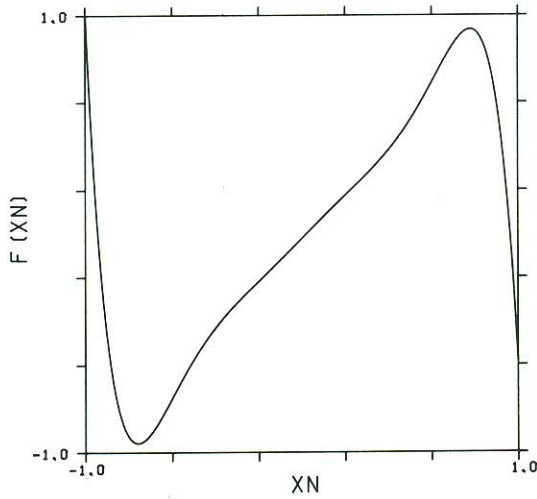


Fig. 12. Iterative map for $a = 0.03$, $b = 4.4$, $c = -6.0$, $e = 0.01$.

Nevertheless, the interpretation above has been confirmed by constructing a one-dimensional return map, which completely reproduces the dynamics reported so far.

5. Equivalent iterative map

To gain a better understanding of the global characteristics of the bifurcation trees found here we built up a one-dimensional iterative map with

a shape similar to that observed in the actual return maps found in the oscillator.

In fact we have chosen a map with inversion symmetry and a fixed point in $x = 0$, that should represent the periodic T solution. The symmetry guarantees the existence of period doubling bifurcations as soon as the slope at $x = 0$ becomes higher than -1 in modulus. Moreover, the map should allow for the existence of two other fixed points that in its second iteration would build up the inverse saddle-node bifurcation. Finally it

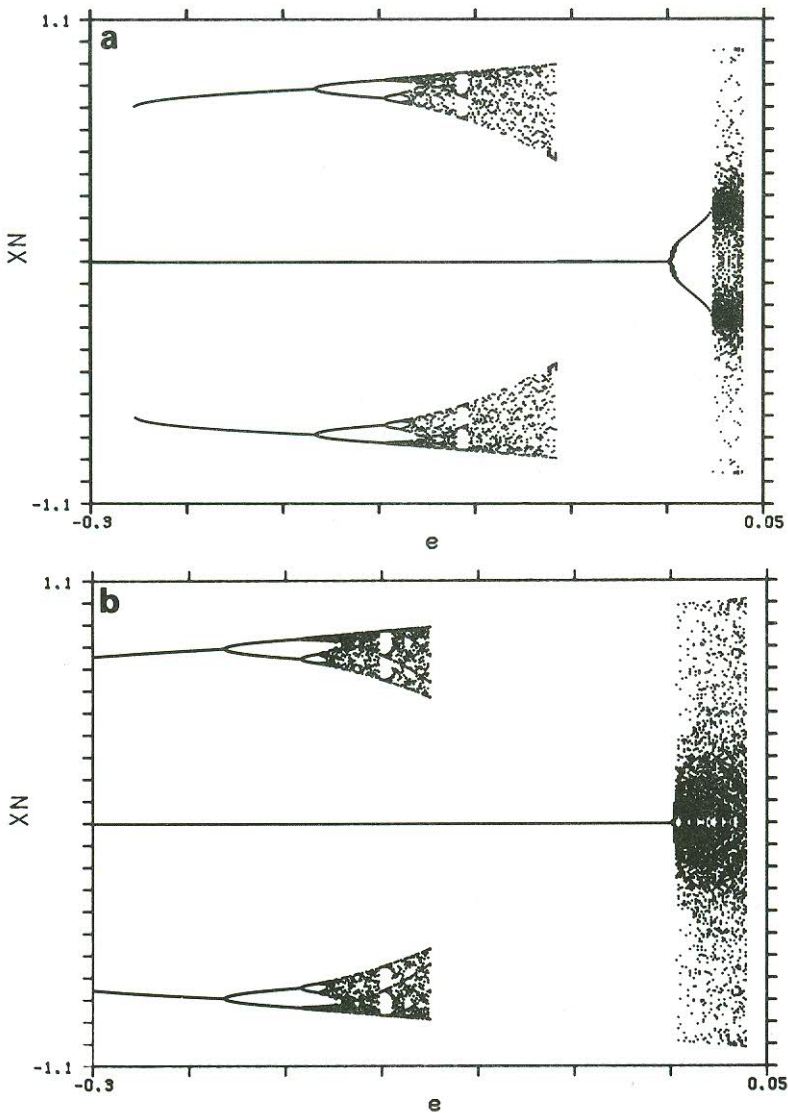


Fig. 13. Bifurcation maps for parameter sets S1 (a) and S3 (b).

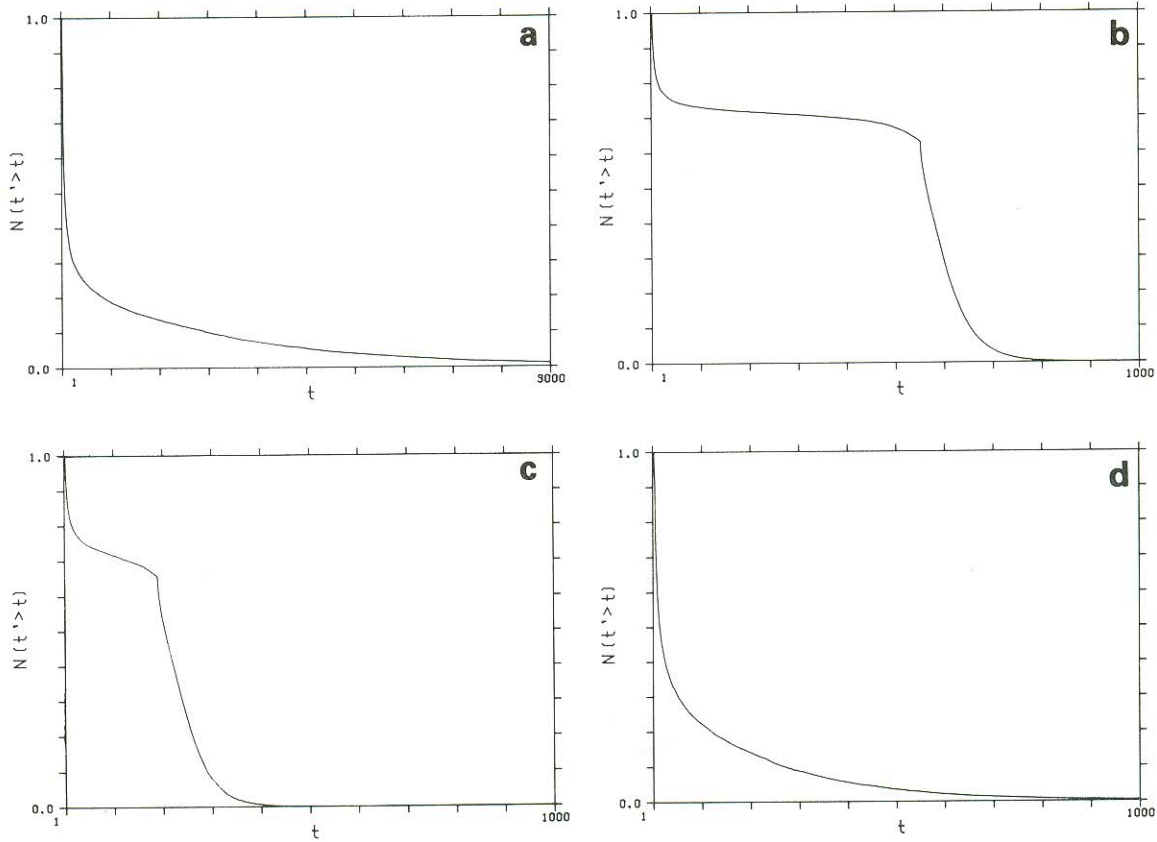


Fig. 14. $N(t \geq t')$ for the map. (a) Parameter set S3, $e = 0.001$; (b), (c) and (d) parameter set S1 and $e = 0.0235$, $e = 0.025$ and $e = 0.052$, respectively.

should allow for reinjection and also for escape to infinity for high values of the control parameter.

All these requirements are fulfilled by a seventh order polynomial map of the form

$$x_{n+2} = (1 + e)x_n + ax_n^3 + bx_n^5 + cx_n^7.$$

The general structure of the map is always similar to that in fig. 12, which is obtained for the following set of parameters: $a = 0.03$, $b = 4.4$, $c = -6.0$, $e = 0.01$. For this map the whole dynamics of the Helmholtz oscillator here reported can be obtained. Let us show the bifurcation diagrams for two different sets of parameter values and using e as bifurcation parameter, considering that the corresponding first iteration of the map has negative linear term coefficient.

Fig. 13(a) corresponds to the set of values $a = -0.746$, $b = 6.5$, $c = -7.8$, that we will label as set S1, while fig. 13(b) corresponds to $a = 0.03$, $b = 4.4$ and $c = -6.0$, and stands for set S3.

It is clear that both bifurcation diagrams display the main features shown in figs. 4 and 7. We can recognize the subcritical period doublings with their complete cascade, and the subsequent destabilization of the respective T - and $2T$ -periodic orbits going into intermittent regimes of type-I and type-III.

The shape of the second iterate return map just over the intermittent transition for the set S1 has the same aspect as the one shown in fig. 12, and the analysis of the statistics confirms the close correspondance between the map and the Helmholtz oscillator.

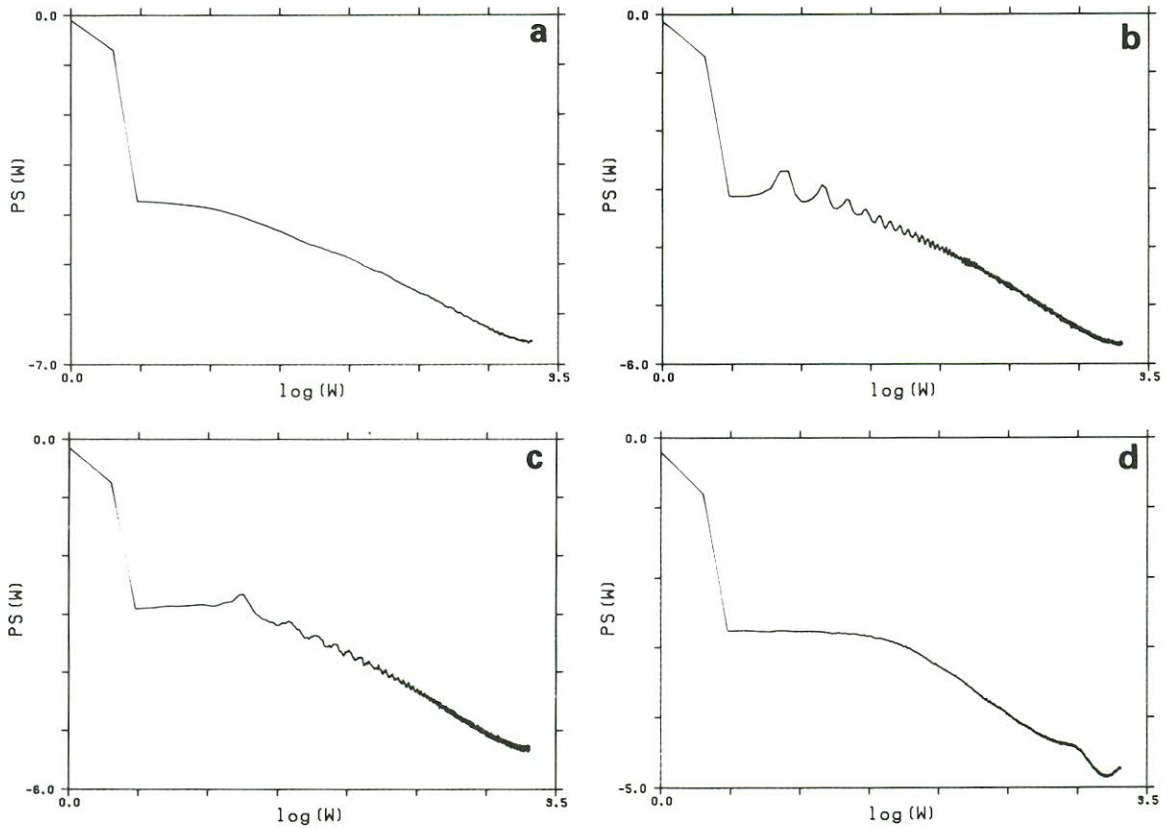


Fig. 15. Power spectrum for the map. Parameter set S1; $e = 0.02318$ (a), $e = 0.0235$ (b), $e = 0.025$ (c) and $e = 0.052$ (d).

In fact the functions $N(t \geq t')$ corresponding to both types of intermittent behavior in the map are depicted in figs. 14(a) to (d). In fig. 14(a) we have plotted the statistics corresponding to the set S3, which yields the type-III intermittent regime, very close to the bifurcation point ($e = 0.0001$). It shows a clear type-III behavior.

Instead, in figs. 14(b) to (d) we have plotted $N(t \geq t')$ for the set S1, for different values of e . It is clear that the global shape of the statistics change from a type-I structure to a type-III one.

Finally this change is also seen in the power spectra of the time series generated by the map. For the set S3, the low-frequency part of the spectrum shows a slope around -1 and fairly independent of e . On the contrary, for the set S1 there is a clear change in the slope when e is varied (figs. 15(a) to (d)).

In fact this slope of the power spectrum changes from a value of 1.4 for $e = 0.02318$ – i.e., very close to the bifurcation point – to 1.18 for $e = 0.052$, where the statistics reveal a shape very similar to that of type-III intermittency. The ripple characteristic of the type-I intermittent regime can also been seen in figs. 15(a) and 15(b).

6. Conclusions

6.1. Main results

We have performed analog and numerical simulations on a nonlinear driven and damped oscillator with quadratic nonlinearity, i.e., with a single-well asymmetric potential. Here we summa-

size the main results of this investigation:

1) The analog simulation allowed us to locate an intermittent zone in parameter space in which $1/f$ noise was present. However we could not decide whether this intermittent transition corresponded to type-I or type-III.

2) By means of the numerical integration we found two different intermittent behaviors in parameter space. Furthermore a continuous parameter change lead from one type of bifurcation (inverse saddle-node) to the other (subcritical period doubling).

3) By means of Floquet multipliers and statistical properties both regimes have been unambiguously classified as pertaining to type-I and type-III intermittencies. Moreover, for the type-I region, we have shown that upon increasing the forcing beyond the bifurcation point, the features of this regime change approaching those of type-III.

4) A monotonic change in the slope of the low-frequency part of the power spectra has been observed. The explanation for this anomalous behavior has been found in the competition between two unstable fixed points.

5) Finally, an iterative map has been introduced that reproduces the whole dynamics of the system in this region of parameter space.

6.2. Discussion

We should make a brief comment on the possible relevance of these conclusions on the problem of labeling an intermittent experimental signal as belonging to type-I or type-III.

The only precise way for classifications of an intermittent signal is by studying the behavior of the Floquet multipliers in the bifurcation. Unfortunately these studies cannot be performed on experimental signals and therefore one is forced to test some other properties that characterize an intermittent regime, such as the statistics or the power spectrum. When this analysis is carried out the situation may appear quite complicated.

For instance in the Helmholtz oscillator we have shown that in a small region of parameter

space both types of intermittency can be found. Indeed, on certain regions, the behavior of the system may appear as belonging to either type depending on the proximity to the bifurcation point. In our case, the behavior may appear to belong to different types of intermittency for points of parameter space separated by 0.002.

Acknowledgements

The authors acknowledge fruitful discussions with Profs. H. Haken, E. Holzhauer, J. Tredicce, M.G. Velarde and Dr. H. Bunz and access to unpublished research results. They would also like to acknowledge hospitality at I.N.O. (Florence, Italy) (M.A.R.) under a NATO Grant, and at Los Alamos Nat. Lab. (Los Alamos, NM, USA) (J.C.A.).

References

- [1] P. Bergé, Y. Pomeau and Ch. Vidal, *L'Ordre dans le Chaos* (Hermann, Paris, 1984).
- [2] H.L. Swinney, N.B. Abraham and J.P. Gollub, *Physica* D11 (1984) 252.
- [3] *Physica Scripta*, T 9 (1985).
- [4] M.J. Feigenbaum, *J. Stat. Phys.* 21 (1979) 669.
- [5] P. Manneville and Y. Pomeau, *Physica* D1 (1980) 219.
- [6] M.J. Feigenbaum, L.P. Kadanoff and S.J. Shenker, *Physica* D 5 (1982) 370.
- [7] J. Crutchfield, D. Farmer, N. Packard, R. Shaw, G. Jones and R.J. Donnelly, *Phys. Lett.* A 76 (1980) 1.
- [8] B.A. Huberman and A.B. Zisook, *Phys. Rev. Lett.* 46 (1981) 626. J.D. Farmer, *Phys. Rev. Lett.* 47 (1981) 179.
- [9] P. Manneville, *J. Physique* 41 (1980) 1235.
- [10] A. Ben Mizrachi, I. Procaccia, N. Rosenberg, A. Schmidt and H.G. Schuster, *Phys. Rev. A* 31 (1985) 1830.
- [11] F.T. Arecchi, R. Badii and A. Politi, *Phys. Rev. A* 32 (1985) 402.
- [12] F.T. Arecchi, R. Meucci, G.P. Puccioni and J. Tredicce, *Phys. Rev. Lett.* 49 (1982) 1217.
- [13] (a) F.T. Arecchi and F. Lisi, *Phys. Rev. Lett.* 49 (1982) 94.
(b) F.T. Arecchi and A. Califano, *Phys. Lett. A* 101 (1984) 443. (c) F.T. Arecchi and A. Califano, *Europhys. Lett.* 3 (1987) 5.
- [14] R.F. Miracky, M.H. Devoret and J. Clarke, *Phys. Rev. A* 31 (1985) 2509.
- [15] E.G. Gwinn and R.M. Westervelt, *Phys. Rev. Lett.* 54 (1985) 1613.

- [16] J. Guckenheimer and P. Holmes, *Nonlinear Oscillations, Dynamical Systems, and Bifurcations of Vector Fields* (Springer, Berlin, 1983).
- [17] H. Helmholtz, *Die Lehre von den Tonempfindungen als Physiologische Grundlage fur die Theorie der Musik* (Friedrich Vieweg, Braunschweig, 1870).
- [18] T. Poston and I. Stewart, *Catastrophe Theory and its Applications* (Pitman, London, 1978).
- [19] J.M. Thompson, S.R. Bishop and L.M. Leung, *Phys. Lett. A* 121 (1987) 116.
- [20] E. Rauchle and E. Holzhauer, private communication and report at an Int. Conf. on Synergetics (unpublished), Schloss-Elmau, West Germany (May 1984).
- [21] R.M. May, *Nature* 261 (1976) 459.
- [22] P. Manneville, in: *Symmetries and Broken Symmetries*, N. Boccara, ed. (I.D.S.E.T., Paris, 1981), p. 517.
- [23] P. Richetti, F. Argoul and A. Arneodo, *Phys. Rev. A* 34 (1986) 726.
- [24] A.H. Nayfeh and D.T. Mook, *Non-linear Oscillations* (Wiley, New York, 1979).
- [25] M. Dubois, M.A. Rubio and P. Bergé, *Phys. Rev. Lett.* 51 (1983) 1446.
- [26] H.G. Solari, E. Eschenazi, R. Gilmore and J.R. Tredicce, *Opt. Commun.* 65 (1987) 47.
- [27] H. Bunz, H. Ohno and H. Haken, *Z. Phys. B* 56 (1984) 345.
- [28] Y. Pomeau and P. Manneville, *Commun. Math. Phys.* 74 (1980) 189.
- [29] J.E. Hirsch, B.A. Huberman and D.J. Scalapino, *Phys. Rev. A* 25 (1982) 519.